

# Dynamic control by sinusoidal perturbation and by Gaussian noise of a system of two nonlinear oscillators: Computation and experimental results

C. P. Cristescu and Cristina Stan

*Department of Physics, Polytechnic University of Bucharest, 313 Spl. Independentei, RO-060042 Bucharest, Romania*

D. Alexandroaei

*Department of Plasma Physics, Al. I. Cuza University of Jassy, 11 Carol 1st Boulevard, 6600-Jassy, Romania*

(Received 9 December 2003; published 29 July 2004)

In this paper we report numerical and experimental studies of the dynamic control of the inter-anode plasma of a double electrical discharge and of a system of two coupled nonlinear oscillators modeling this plasma. We compare the transition between chaotic dynamics and periodic dynamics induced by a sinusoidal perturbation and by small-dispersion Gaussian noise. Besides considerable differences between the effect of the two types of perturbation we also find important similarities. For small amplitude, both the sinusoidal and the white noise perturbations can induce the system to change from chaotic to regular dynamics. In the case of sinusoidal perturbation, the transition time from the chaotic to regular state has a definite duration that depends on the values of the perturbation parameters. The suppression of the perturbation has no influence on the state — the system remains in the same regular state. Subsequent reinstatement of the same type of perturbation with the same amplitude does not change the periodic state of the system but, for considerably higher amplitude, the system is switched back to its chaotic state. For moderate-amplitude sinusoidal perturbation, intermittent transitions between the chaotic and regular states is observed. Most of these predictions of the model have been observed experimentally in a system of two coupled electrical discharges. Our results suggest practical methods that can be used for controlling the discharge plasma dynamics.

DOI: 10.1103/PhysRevE.70.016613

PACS number(s): 05.45.Yv, 52.35.-g, 05.40.-a

## I. INTRODUCTION

In recent years, dynamic control of nonlinear systems has become a challenging subject in various interdisciplinary fields. Numerical simulation and experimental methods were reported in physical, chemical, and biological systems with major impact on many aspects of science and engineering [1–10]. A lot of theoretical and experimental work is dedicated to phase synchronized chaos [11–16] and also to lag synchronization [17]. In addition to the synchronization of mutual chaotic oscillators, coupled nonlinear oscillators exhibit a diversity of fundamental dynamical phenomena when the nonlinearity or the coupling strength is increased.

The plasma of electrical discharges is a highly nonlinear system that performs a variety of nonlinear oscillations. The study of nonlinear nonequilibrium phenomena in such extended systems is one of the most active areas of research [18–21]. It is demonstrated that many of these oscillatory phenomena are related to spatial charge structures (SCS's) generated according to a self-organized scenario [22].

Since for some applications purely harmonic oscillations are required, it is necessary to suppress the higher harmonics or to change the chaotic behavior into a periodic one. This is possible by controlling the discharge with an external circuit [23]. Also, because of the strong nonlinearity of the SCS's formed in plasma, the intrinsic noise in the system can induce uncorrelated oscillations of the current, corresponding to jumps of the structure between various states. Since it is very difficult to control the internal noise level experimentally, an alternative is to inject noise that can be controlled from outside. The effect of additive noise on chaos control has been the subject of our recent numerical and experimental investigation [24]. Depending on the relation between the

characteristics of the external circuit (frequency and amplitude) and the parameters of the plasma oscillations, different types of synchronization, periodic pulling, period doubling bifurcations, and chaos were reported [25–30].

This study is a consequence of experimental measurements carried out on the oscillations of the plasma generated in the interanode space of a double-plasma-discharge system. It was found that the nonlinear phenomena are related to the dynamics of SCS's — in the form of double layers—and that various nonlinear dynamics observed are satisfactorily reproduced by a system of equations [28,29] representing a modified version of two bidirectionally coupled van der Pol oscillators modeling individually the two discharges.

In this work we present the effect of the sinusoidal perturbation on the dynamics of the model system with identical nonlinearity in two situations: for very small amplitude (a few percent of the average amplitude of the free oscillation of the system) and for relatively large amplitude (representing an important fraction of the amplitude of the system). We compare the results with the effect obtained by replacing the sinusoidal perturbation with Gaussian noise. Besides considerable differences between the two possibilities of dynamic control we also find important similarities. Most of the predictions of the model have been observed experimentally in a system of two coupled electrical discharges.

## II. EXPERIMENTAL SETUP AND COMPUTATIONAL MODEL

A detail of the experimental setup used is shown in Fig. 1. For further details, see [29]. The two adjacent glow discharges  $K_1A_1$  and  $K_2A_2$  run independently between the plane

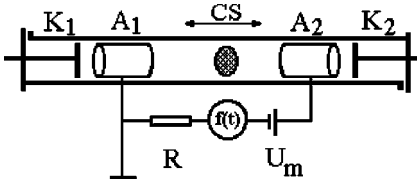


FIG. 1. A detail of the experimental setup.

cathodes  $K_1$ ,  $K_2$  and the cylindrical anodes  $A_1$ ,  $A_2$ . The anodes are biased one with respect to the other by the dc source  $U_m$  and the perturbation  $f(t)$  is connected in series with  $U_m$ . Here,  $f(t)$  is either a sinusoidal voltage generator or a white noise voltage generator. The flowing working gas is argon at a pressure around 0.2 Torr and the parameters of the individual discharges have values typical for glow discharges. The oscillations of the discharge current flowing between the two anodes were recorded as a voltage drop on the load resistor  $R$  using a digital data acquisition technique. We study the dynamics of the charge structures formed in the interanode region (denoted CS in Fig. 1) as reflected in the temporal behavior of the current flowing between the two anodes.

The various nonlinear dynamics observed in the behavior of the double-electrical-discharge plasma are satisfactorily reproduced by the following model system of equations [24,29]:

$$\dot{x}_1 = x_2 + mx_4, \quad (1)$$

$$\dot{x}_2 = -c(x_1^2 - 1)x_2 - x_1 + f(t) + mx_4 + (m - n)x_3 + qm, \quad (2)$$

$$\dot{x}_3 = x_4 - mx_2, \quad (3)$$

$$\dot{x}_4 = -d(x_3^2 - 1)x_4 - x_3 + f(t) - mx_2 - (m - n)x_1. \quad (4)$$

In the case of sinusoidal perturbation

$$f(t) = e \cos x_5, \quad (5)$$

and an additional equation  $\dot{x}_5 = 2\pi g$ , with  $g$  the frequency of the perturbation, is added to the system (1)–(4) for making it autonomous.

As random perturbation, we consider a stationary Gaussian noise characterized by zero mean and  $\delta$  correlated in time:

$$f(t) = \psi(t), \langle \psi(t) \rangle = 0, \langle \psi(t) \psi(t') \rangle = 2\sigma^2 \delta(t - t'), \quad (6)$$

where  $\sigma$  is the standard deviation,  $\sigma^2$  being considered as a measure for the noise intensity.

The model can easily be recognized as a modified version of a system of two coupled van der Pol oscillators modeling individually the two discharges. They are coupled by a dc biasing on which a small sinusoidal or white noise voltage is superimposed. The dc biasing is modeled by the parameter  $m$ , which in this study plays the role of control parameter. We consider the effect of these perturbations on the dynamics of the model system with identical nonlinearity of the two oscillators ( $c=d=1$ ) but slightly different values of these parameters give essentially the same results [29]. The constant

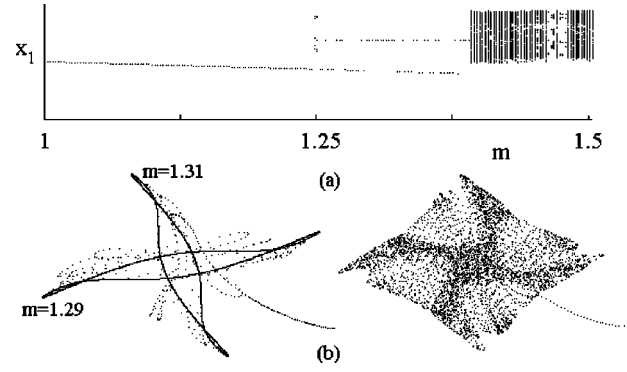


FIG. 2. (a) Bifurcation diagram for  $x_1$ . The initial conditions are  $x_1=10$ ,  $x_2=x_3=x_4=0$ . (b) Phase portrait projected on the  $(x_1, x_3)$  plane: left, limit cycles for  $m=1.29$  and  $m=1.31$ ; right, chaos for  $m=1.41$ .

$n$  takes into consideration the fact that the mutual interaction between the oscillators is smaller than the self-coupling rate. The constant  $q$  stands for the slight asymmetry between the two discharges. The values used in the present simulation are  $n=0.01$  and  $q=0.01$ .

### III. PERTURBATION WITH SINUSOIDAL SIGNAL

First, we present the behavior of the system free of any perturbation. This is most conveniently observed from the bifurcation diagram for  $x_1$  shown in Fig. 2(a) for a certain choice of initial conditions [32,33]. For values of the control parameter below  $m=1.35$ , the dynamics of the system consists of periodical oscillations. For  $m$  in excess of this value, the dynamical characteristics change into a chaotic regime. In the range of periodic behavior, the system can evolve to a stable state (limit cycle) for  $m < 1.25$  or to one of a pair of stable states (for  $m > 1.25$ ).

In the latter case, for an established set of initial conditions, access to one or the other of the two states is decided by the value of the control parameter (the coupling between the oscillators). This is illustrated in Fig. 2(b), which shows the phase portrait projected on the  $(x_1, x_3)$  plane, on the left, the situation corresponding to the two stable limit cycles (for  $m=1.29$  and  $m=1.31$ ) and, on the right, the chaotic oscillations corresponding to values of  $m$  in excess of  $m=1.4$ .

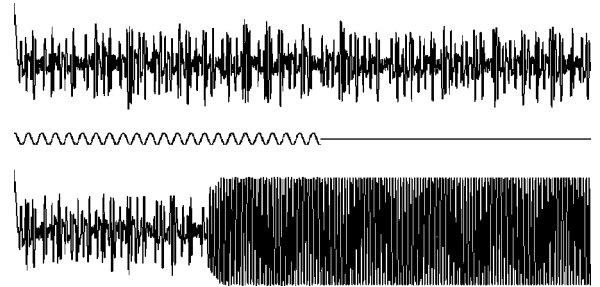


FIG. 3. Upper trace: time series  $x_1(t)$  in the free (unperturbed) evolution of the system. Middle trace: the perturbation. Bottom trace: time series  $x_1(t)$  in the presence of the perturbation shown by the middle trace.

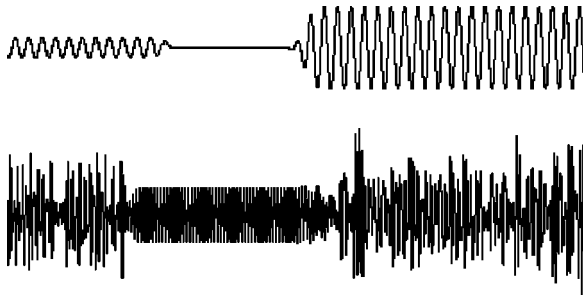


FIG. 4. Upper trace: perturbation removed and reinstated later. Bottom trace: time series  $x_1(t)$  in the presence of the perturbation shown by the upper trace. Reinstatement of the same perturbation, but with considerable larger amplitude, throws the system back to chaotic dynamics.

For a given value of  $m$ , the state of choice depends on the initial conditions. In one of these states, the amplitude of the first oscillator  $x_1$  is large and the amplitude of the second oscillator  $x_3$  is small and vice versa in the other [Fig. 2(b), left]. The structure of the spectrum of free oscillation is similar to that shown in Figs. 5(b) and 5(c). The only difference between the spectra corresponding to the two states consists in the energy distribution between the fundamental and its harmonics. In the large-amplitude state, the oscillation is closer to sinusoidal (the ratios of the amplitude of the harmonics over the fundamental are very small). In the other state the fundamental frequency is the same but the energy distribution is more in favor of the harmonics.

These results show that in the phase space of the system, between the two stable dynamical equilibrium states a chaotic attractor exists and also that the spatial separation between this chaotic attractor and the two limit cycles is not very large.

The sinusoidal perturbation is considered in two situations: for very small amplitude ( $e$ , a few percent of the average amplitude of the free oscillation of the system) and for relatively large amplitude (representing an important fraction, above 30% of the amplitude of the unperturbed oscillation). For amplitudes of the sinusoidal perturbation below 3% of the amplitude of the unperturbed system the chaotic behavior persists. Also, for amplitudes in the interval 15% – 25% no transition to a regular state was observed.

In the case of small-amplitude perturbation, we consider an interval of values of the control parameter  $m$  in excess of

1.39, where the behavior of the unperturbed system is chaotic, as shown by the bifurcation diagram on Fig. 2(b).

The effect is clearly visible in Fig. 3. Here, the upper trace is the time series  $x_1(t)$  in the free (clearly chaotic) evolution of the system. The bottom trace represents the same time series in the presence of the perturbation shown by the middle trace. We mention that the amplitude of the perturbation and the amplitude of  $x_1$  in Fig. 3 are not represented at the same scale — the middle trace amplitude is only 3% of the lower trace amplitude. In the presence of perturbation, the system evolves towards a periodic state after a certain time, always the same for fixed parameters of the perturbing signal (amplitude and frequency), but different for different values of the parameters. We should emphasize that the dependence of this time interval on the values of both the amplitude and frequency of the perturbation is characterized by fractal structure.

As observed from Fig. 3, subsequent removal of the perturbation does not change the periodic dynamics. This shows that the role of the perturbation mainly consists in pushing the trajectory out of the basin of the chaotic attractor and into the basin of a periodic attractor which is in very close proximity with the chaotic one.

If the perturbation is reinstated with the same amplitude, the system remains in the same regular state. Reinstated perturbation with an amplitude 5–6 times larger is necessary to push the system back to the chaotic state, demonstrating that the periodic state once reached is robust. This behavior is presented in Fig. 4.

The situation discussed is well illustrated by the spectra shown in Figs. 5(a)–5(c). The spectrum in Fig. 5(a) corresponds to the chaotic time series (upper trace on Fig. 3), while the spectra in Figs. 5(b) and 5(c) correspond to periodic states obtained with perturbing signals of the same amplitude but with different frequencies (marked by the vertical arrow in each figure). Irrespective of the perturbation frequency, the system is always pushed to the same state, characterized by the frequency of the free oscillation.

The situation is entirely different for perturbation of large amplitude (around 30% of the amplitude of the free oscillation of the system). This is clearly observed from the bifurcation diagrams shown in Fig. 6 for three different values of the amplitude  $e$  as shown on each graph.

We choose a different way of presenting the dynamics. For most of the range of control parameters investigated, the

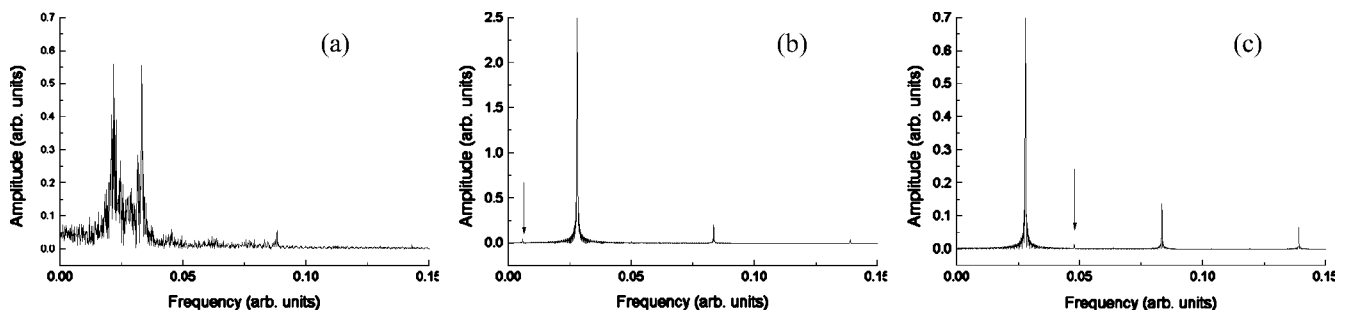


FIG. 5. The spectra correspond to (a) chaotic time series (upper trace in Fig. 3), (b) periodic states obtained with perturbing signal with frequency (marked by the arrow) smaller than the free oscillation frequency, and (c) periodic states obtained with perturbing signal with frequency (marked by the arrow) larger than the free oscillation frequency.

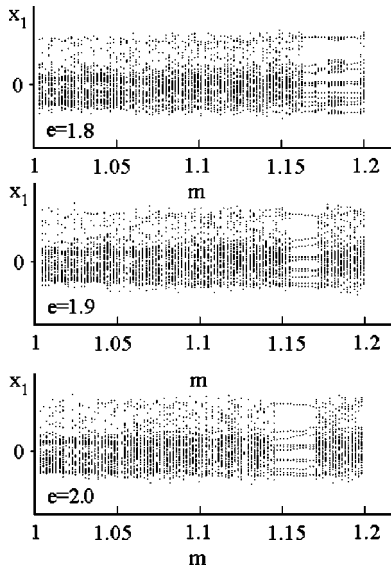


FIG. 6. Bifurcation diagrams for  $x_1$  in the presence of perturbation with various amplitude marked by the value of  $e$  in each graph.

perturbation has the opposite effect as compared with that of small-amplitude perturbation—namely, to push the trajectory out of the basin of the periodic attractor and into the basin of the chaotic attractor. However, there are very small intervals of values of the control parameter for which the system synchronizes on frequencies determined by the perturbation frequency, mainly subharmonics thereof. The position and range of the periodic windows strongly depend on the parameters of the perturbation. This is most conveniently observed by a stroboscopic investigation at frequency  $g$  as

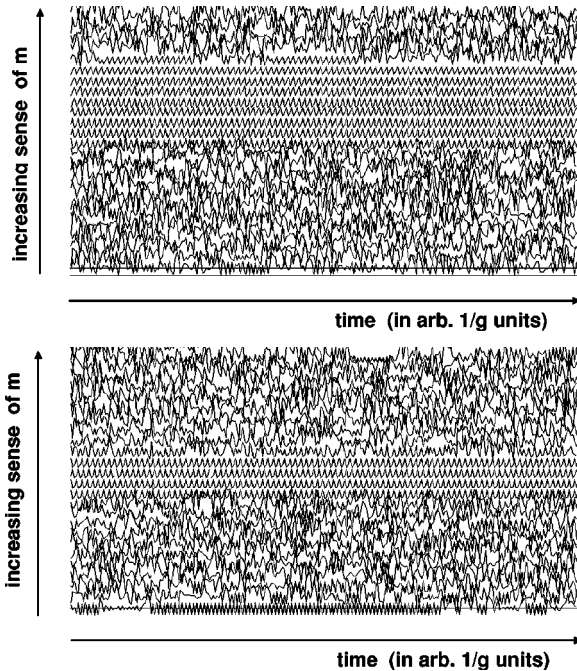


FIG. 7. Time series  $x_1=x_1(t)$  stroboscopically taken during the uniform variation of the control parameter  $m$  in steps of 0.005 for two different amplitudes  $e$  of the perturbing force:  $e=1.8$ ,  $m_{initial}=1.1$  (upper picture);  $e=1.9$ ,  $m_{initial}=1.1$  (lower picture).

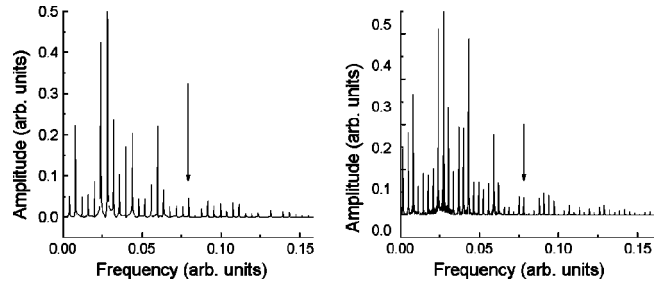


FIG. 8. Spectra corresponding to two different values of the perturbation parameters, the same as in Fig. 7, for  $m=1.17$ ,  $e=1.9$  (left);  $m=1.19$ ,  $e=1.8$  (right). The frequency of the perturbation is marked by the arrows.

shown by the diagrams in Fig. 7 for values of the amplitude  $e=1.8$  and  $e=1.9$ . This type of investigation is better than the bifurcation diagram because it allows the observation of intermittent dynamics, which on the conventional bifurcation diagram appears as chaotic. This is clearly observed in one of the time series in the upper graph.

The spectra corresponding to the same values of the perturbation parameters as in Fig. 7 are shown on Fig. 8 for  $m=1.17$ ,  $e=1.9$  (left) and  $m=1.19$ ,  $e=1.8$  (right). Here, the arrows mark the perturbation frequency. Slightly different frequencies (equal amplitudes) generate considerably different spectra.

For intermediate values of the perturbation amplitude (in the neighborhood of 20% of the amplitude of the free oscillation) the system can be intermittently entrained by the perturbation, as clearly seen from Fig. 7.

#### IV. PERTURBATION WITH GAUSSIAN NOISE

In the case of perturbation by noise, the function  $f(t)$  in the system (1)–(4) is defined by Eqs. (6). The Gaussian noise is generated according to the Box-Muller algorithm [31]. We consider values of the noise amplitude  $\sigma$  in the range 0.01–0.2, which represents less than 5% of the amplitude of the free oscillations of the system.

By contrast to the situation with small-amplitude sinusoidal perturbation, where for fixed values of the perturbation parameters ( $e, g$ ) the duration of the evolution of the

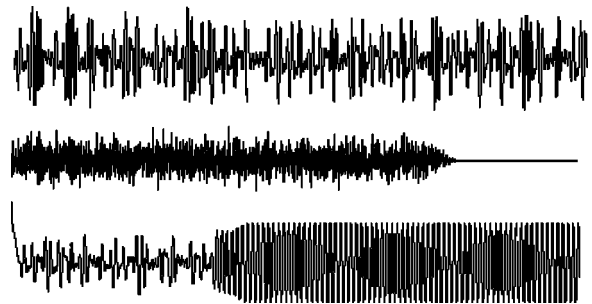


FIG. 9. Upper trace: time series  $x_1(t)$  in the free (unperturbed) evolution of the system. Middle trace: the perturbation, Gaussian noise. Bottom trace: time series  $x_1(t)$  in the presence of the perturbation shown by the middle trace.



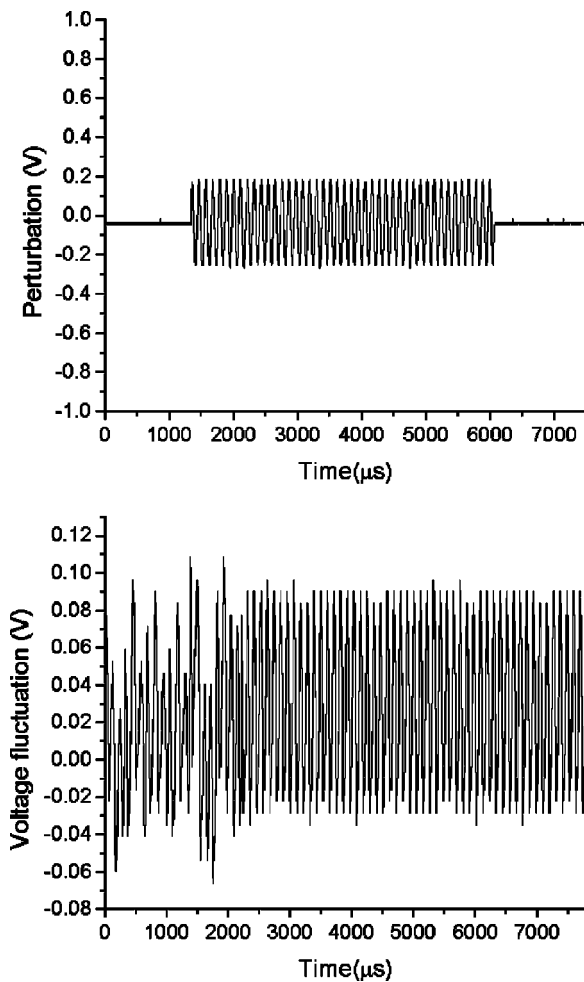


FIG. 10. Upper graph: on and off application of the low-amplitude perturbation from the external sinusoidal signal generator. The bottom graph: simultaneous fluctuations of the interanode current measured as voltage fluctuations on a load resistor.

system from chaos to periodic oscillation is entirely predictable, here, as expected, no prediction is possible. In the range of noise intensity where transition from the chaos to periodic state is observed, the system ends up in one or the other of its two stable states. Similar results were obtained when a uniform random noise is used instead of the Gaussian noise. After the transition, the removal of the noise is not changing the state of the system, as shown in Fig. 9.

Reinstatement of noise with the same or slightly larger intensity has no effect on the periodic state. However, reinstatement of a noise with considerably larger intensity throws the system back into the chaotic state.

## V. EXPERIMENTAL RESULTS

In this section we present experimental results on the effect of small-amplitude sinusoidal perturbation and preliminary results on the synchronization with Gaussian noise. Experimental results on the synchronization with large-amplitude sinusoidal perturbation (forcing) were extensively presented in previous works [28–30].

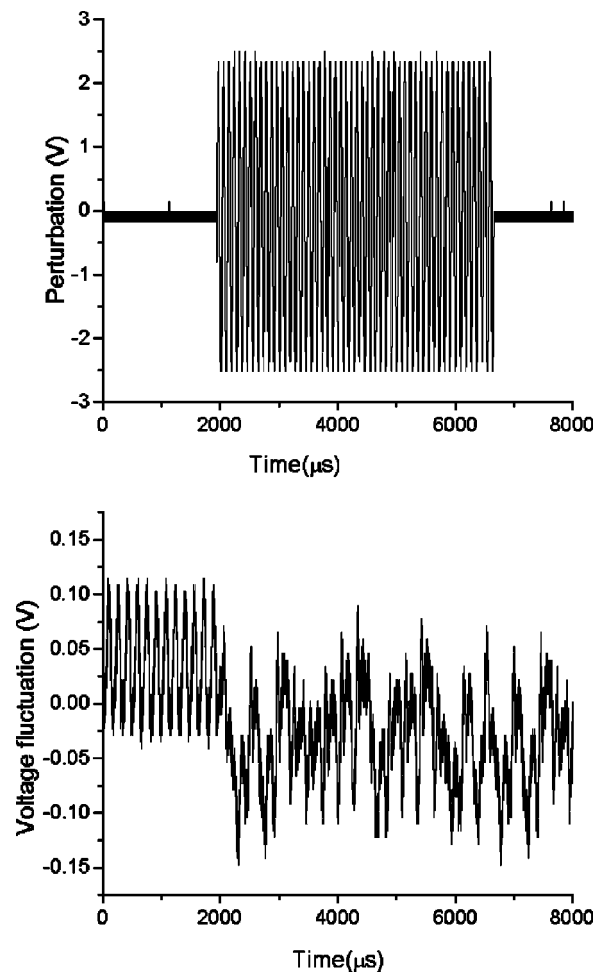


FIG. 11. Upper graph: on and off application of the higher-amplitude perturbation from the external sinusoidal signal generator. The bottom graph: simultaneous fluctuations of the inter-anode current measured as voltage fluctuations on a load resistor.

For sinusoidal perturbation of smaller amplitude, we managed to obtain an experimental behavior close to that predicted by the computational model and shown in Figs. 3 and 4. The experimental results for the biasing voltage  $U_m = 41$  V are presented in Figs. 10 and 11.

The upper graph in both figures shows the sinusoidal perturbation from the external signal generator that is turned on and then turned off after a certain time. In Fig. 10 the amplitude of the perturbation is considerably smaller than in Fig. 11. The lower graphs in both pictures show the fluctuation of the interanode current measured as the voltage drop on the load resistor. The bottom graph in Fig. 10 demonstrates that the system, initially in a chaotic state, is pushed to a regular state and remains in this state after the switching off of the perturbation. This behavior is in agreement with the predicted situation presented in Fig. 3.

The bottom graph in Fig. 11 shows that the system initially in a periodic state is desynchronized by a perturbation of higher amplitude and remains in the chaotic state after the switching off of the perturbation. This behavior is in agreement with the predicted situation presented in Fig. 4. The small jump in the average current that appears on application

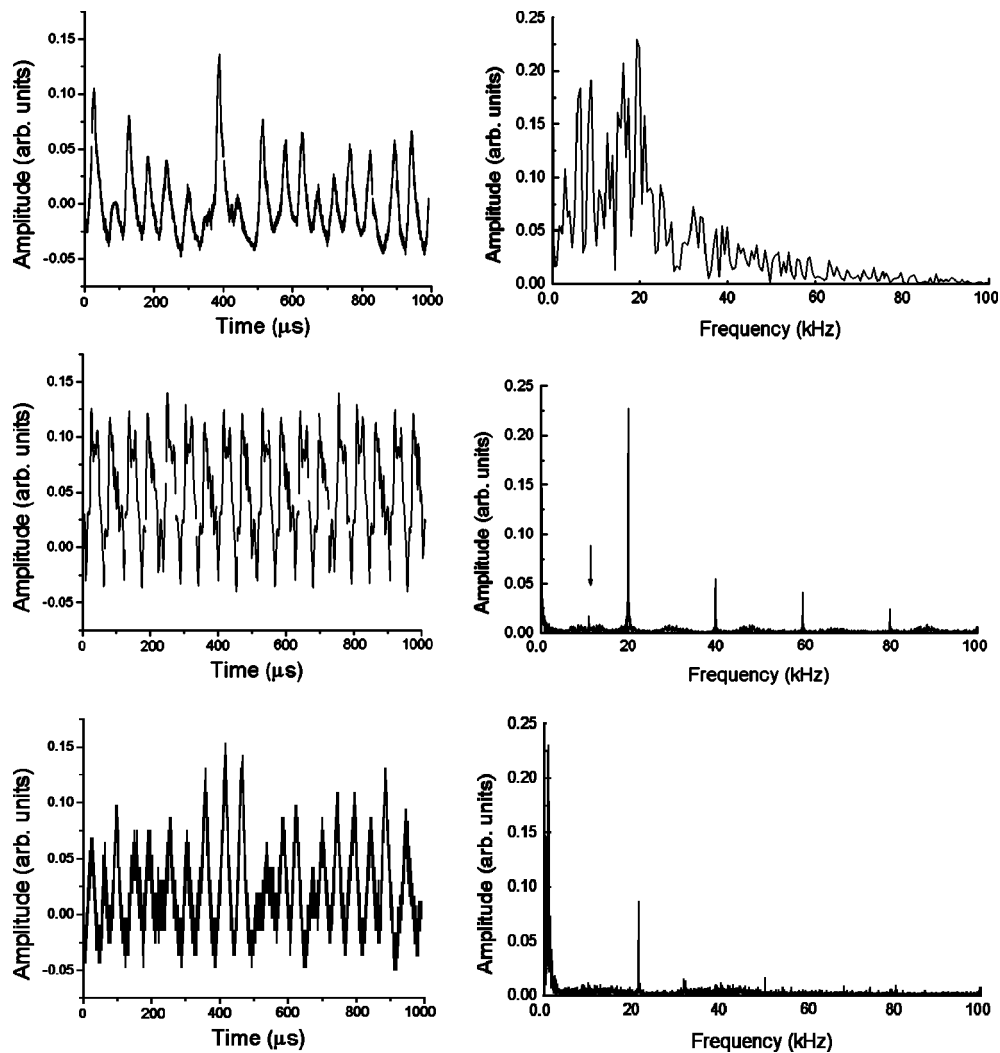


FIG. 12. Time series (left) and fast Fourier transform (FFT) spectra (right): upper graphs, chaotic behavior for free running of the system; middle graphs, running under small amplitude (10%) sinusoidal perturbation with the frequency marked by the arrow in the FFT spectrum; lower graphs, running with small-amplitude white Gaussian noise with an equivalent standard deviation  $U_s=10$  V rms and 20-fold attenuation. The results correspond to the same biasing  $U_m=41$  V.

of the perturbation is caused by a sudden change in the dynamics of the electrical discharge (disruption of the charge structures).

So far, for Gaussian noise, we were unable to observe the effect in the time series as clearly as in the case of sinusoidal perturbation. However, a transition to the periodic state induced by small-amplitude Gaussian noise was observed using spectral analysis, as shown in Fig. 12. Here, the time series (left) and FFT spectra (right) for three experimental situations are presented. The upper graphs refer to the free running of the system in conditions of chaotic behavior for a value of the dc biasing potential  $U_m=41$  V. The middle graphs correspond to running under small-amplitude (10%) sinusoidal perturbation with the frequency marked by the arrow in the FFT spectrum, for the same value of the dc biasing. The lower graphs represent the transition from chaos to periodic dynamics obtained under a small-amplitude white Gaussian noise and the same biasing. We use a noise signal generator with an equivalent standard deviation of  $U_s=10$  V rms, coupled to the discharge system through an at-

tenuation network. The lower graphs in Fig. 12 correspond to a noise level  $U_s/20$ . It should be observed that in the case of perturbation by noise, beside the main frequency, the same as in the case of sinusoidal perturbation (about 20 kHz), another spectral component at much lower frequency is promoted. This behavior seems to indicate a stochastic resonance phenomenon and is one of our interests for further investigations.

For moderate noise amplitude ( $U_s/5$ ), the change induced in the behavior of the system is different. We did not manage to obtain a transition to the periodic state at this noise level for the above values of the system parameters. For lower values of the biasing, where the system behaves regularly, a higher-level noise usually induces transitions from periodic dynamics to chaotic ones.

The physical mechanism of the transition between chaotic and regular dynamics is correlated to the dynamics of SCS's such as intermittent detachment of the double layer from the SCS and changes in their moving phase [25]. Also it is ob-

served that some moving phase SCS's are more stable against noise than others.

## VI. CONCLUSIONS

The results of dynamic control obtained by a sinusoidal perturbation are compared with the effect obtained with a Gaussian noise signal, both theoretically using a computational model of two perturbed, coupled nonlinear oscillators, and experimentally using a double-discharge plasma system.

Besides considerable differences between the two possibilities of dynamic control we also find important similarities. For small amplitude, both the sinusoidal and white noise perturbations can move the system from a chaotic to a periodic state. In the case of small-amplitude sinusoidal perturbation the transition time has a well-defined value depending on the values of the perturbation parameters. Subsequent re-statement of the same type of perturbation but with higher amplitude switches the system back to its chaotic state.

For large amplitudes, the transition to a regular state cannot be achieved. However, for sinusoidal perturbations, in-

termittent transitions between chaotic and periodic states are obtained.

Most of the computation results presented have been observed experimentally in the fluctuations of the interanode current of a system of the two coupled electrical discharges. Using a small-amplitude sinusoidal perturbation or a small-dispersion Gaussian noise, we changed the behavior of our discharge system from a chaotic state to a periodic state and, most importantly, the periodic state persisted after removal of the perturbation. In the case of a random perturbation, the dynamic control of the experimental system was considerably more difficult. We consider that this could be a consequence of a multiplicative influence between the external and internal noise, always present in the experimental device.

Our results are of practical importance in suggesting methods that can be used for controlling the dynamics of a discharge plasma [34].

## ACKNOWLEDGMENT

This work was partially supported by CERES through Grant No. 3-135/2003.

- 
- [1] E. Ott, E. D. Yorke, and J. A. Yorke, *Physica D* **16**, 62 (1985).
  - [2] E. Ott, C. Grebogi, and J. A. Yorke, *Phys. Rev. Lett.* **64**, 1196 (1990).
  - [3] V. S. Anishchenko, T. E. Vadivasova, D. E. Potsnov, and M. A. Safonova, *Int. J. Bifurcation Chaos Appl. Sci. Eng.* **2**, 633 (1992).
  - [4] M. Kraus, J. Muller, D. Lebender, and F. W. Schneider, *Chem. Phys. Lett.* **260**, 51 (1996).
  - [5] J. N. Weiss, A. Garfinkel, M. L. Spano, and W. L. Ditto, *J. Clin. Invest.* **93**, 1355 (1994).
  - [6] T. Wennekers and F. Pasemann, *Int. J. Bifurcation Chaos Appl. Sci. Eng.* **6**, 2055 (1996).
  - [7] D. J. Christini and J. J. Collins, *Phys. Rev. E* **52**, 5806 (1995).
  - [8] D. J. Christini and J. J. Collins, *Phys. Rev. E* **53**, R49 (1996).
  - [9] R. Breban, *Phys. Rev. E* **68**, 047201 (2003).
  - [10] E. Neumann, I. Sushko, Y. Maistrenko, and U. Feudel, *Phys. Rev. E* **67**, 026202 (2003).
  - [11] M. G. Rosenblum, A. S. Pikovsky, and J. Kurths, *Phys. Rev. Lett.* **76**, 1804 (1996).
  - [12] A. S. Pikovsky, M. G. Rosenblum, and J. Kurths, *Synchronization: A Universal Concept in Nonlinear Sciences* (Cambridge University Press, Cambridge, England, 2001).
  - [13] U. Parlitz, L. Junge, W. Lauterborn, and L. Kocarev, *Phys. Rev. E* **54**, 2115 (1996).
  - [14] J. R. Terry, K. S. Thornburg, Jr., D. J. DeShazer, G. D. Vanwiggeren, S. Zhu, P. Ashwin, and R. Roy, *Phys. Rev. E* **59**, 4036 (1999).
  - [15] D. J. DeShazer, R. Breban, E. Ott, and R. Roy, *Phys. Rev. Lett.* **87**, 044101 (2001).
  - [16] K. Josic and D. J. Mar, *Phys. Rev. E* **64**, 056234 (2001).
  - [17] S. Taherion and Y. C. Lai, *Phys. Rev. E* **59**, R6247 (1999).
  - [18] A. Dinklage, B. Bruhn, H. Deutsch, P. Jonas, B.-P. Koch, and C. Wilke, *Phys. Plasmas* **5**, 833 (1998).
  - [19] T. Mausbach, T. Klinger, and A. Piel, *Phys. Plasmas* **6**, 3817 (1999).
  - [20] T. Klinger, C. Schroder, D. Block, F. Greiner, A. Piel, G. Bonhomme, and V. Naulin, *Phys. Plasmas* **8**, 1961 (2001).
  - [21] T. Klinger, F. Greiner, A. Rohde, A. Piel, and M. E. Koepke, *Phys. Rev. E* **52**, 4316 (1995).
  - [22] R. Schrittwieser, C. Avram, P. C. Balan, V. Pohoata, C. Stan, and M. Sanduloviciu, *Phys. Scr.* **T84**, 122 (2000).
  - [23] V. Pohoata, Ghe. Popa, R. Schrittwieser, C. Ionita, and M. Cercck, *Phys. Rev. E* **68**, 016405 (2003).
  - [24] C. P. Cristescu, C. Stan, and D. Alexandroaei, *Phys. Rev. E* **66**, 016602 (2002).
  - [25] D. Alexandroaei and M. Sanduloviciu, *Phys. Lett. A* **122**, 173 (1987).
  - [26] C. Stan, D. Alexandroaei, and C. P. Cristescu, *Rom. Rep. Phys.* **54**, 185 (2002).
  - [27] C. P. Cristescu, I. M. Popescu, and A. M. Preda, *Rev. Roum. Phys.* **36**, 181 (1991).
  - [28] C. Stan, C. P. Cristescu, and D. Alexandroaei, in *Proceedings of the XXV ICPIG, Nagoya, 2001*, edited by Toshio Goto (University of Nagoya Press, Nagoya, 2001), Vol. 3, p. 169.
  - [29] C. Stan, C. P. Cristescu, and D. Alexandroaei, *Contrib. Plasma Phys.* **42**, 81 (2002).
  - [30] C. Stan, C. P. Cristescu, and D. Alexandroaei, in *Proceedings of the XXVI ICPIG, Greifswald, Germany, 2003*, edited by J. Meichsner, D. Loffhagen, and H.-E. Wagner (Kiebu-Druck, Greifswald, 2003), Vol. 4, p. 185.
  - [31] Athanasios Papoulis, *Probability, Random Variables, and Stochastic Processes*, 3rd ed. (McGraw-Hill, New York, 1991).
  - [32] R. C. Hilborn, *Chaos and Nonlinear Dynamics* (Oxford University Press, New York, 1994).
  - [33] J. M. Aguirregabiria, *Dynamics Solver 2000* (University of the Basque Country, Spain, 2000).
  - [34] M. Sanduloviciu, V. Melnig, and C. Borcia, *Phys. Lett. A* **229**, 354 (1997).